Available online at www.sciencedirect.com

ScienceDirect

Energy Procedia 69 (2015) 573 – 582

Energy Procedia

International Conference on Concentrating Solar Power and Chemical Energy Systems, SolarPACES 2014

Numerical simulation of quartz tube solid particle air receiver

F. Wang[a], F. Bai[a]*, Z. Wang[a], X. Zhang[a]

[a]*Key Laboratory of Solar Thermal Energy and Photovoltaic System, Institute of Electrical Engineering, Chinese Academy of Sciences, Address: 6 Beiertiao, Zhongguancun,Haidian Disctric, Beijing, Postcode:100190,China.*

Abstract

The quartz tube solid particle air receiver is a new type of solar receiver in which fluidized particles absorb the solar radiation directly and heat the air effectively, improving the efficiency of solar thermal power generation and reducing costs. In this article, transient numerical simulation was conducted to simulate the heat transfer and flow processes in single quartz tube under concentrated solar radiation. The results showed that the distribution of solid particles temperature was uniform in the fluidized region, which could overcome the problem of overheating in the volumetric solar receiver. The temperature difference between solid particles and air was no more than 25K, indicating that heat transfer between particles and air was very effective. Further, as the direct solar radiation increased, the average air temperature in the outlet increased while the thermal efficiency decreased. The high tube wall temperature caused heat loss to the environment by radiative and convective heat transfer. With the air inlet velocity increasing, the averaging air temperature in the outlet decreased while the efficiency of the receiver increased. The simulation results provided important reference for improving the performance of the quartz tube solid particle air receiver.

Peer review by the scientific conference committee of SolarPACES 2014 under responsibility of PSE AG

Keywords: solar power generation; quartz tube; solid particles; air receiver; numerical simulation

1. Introduction

Receiver is the key component that affects the efficiency of solar power tower system directly. In order to utilize solar energy more efficiently and lower the cost of solar thermal power plant, more effective thermodynamic cycle

* Corresponding author. Tel.: +86-1082547036.
E-mail address: baifw@mail.iee.ac.cn

Peer review by the scientific conference committee of SolarPACES 2014 under responsibility of PSE AG
doi:10.1016/j.egypro.2015.03.066

should be implemented [1]. Solar particle air receiver in which solid particles absorb the solar radiation and transfer the heat to the flowing air is a promising candidate. Hsieh H-T et al. [2] simulated particle-gas flow within a solid particle receiver and analyzed the factors that could affect the performance of receiver. Nathan P. Siegel et al. [3] developed and evaluated a prototype solid particle receiver. According to their experiment, particles can be heated to more than 900 ^{o}C, which demonstrated that such receiver can be used in practice. However, the above researches mainly focus on falling curtain particle receiver in which the solid particle volume fraction is no more than 3%. In 2013, F. Bai et al. [4] developed and tested a five quartz tubes solid particle air receiver on a solar furnace system with more than 20 % solid particle volume fraction. The approximate solid particle size was 3mm. In this paper, the solid particle air receiver with single quartz tube was simulated numerically by CFD (Computational Fluid Dynamics) software Ansys Fluent 14.0. The results displayed the heat transfer mechanism between solid particles and air in the solar receiver and provided important reference for improving the performance of such air receiver.

Nomenclature

A_{pn}	projected area of solid particle n (m^2)
$C_{1\varepsilon}$##	constant in k-epsilon model
$C_{2\varepsilon}$##	constant in k-epsilon model
$C_{3\varepsilon}$##	constant in k-epsilon model
C_{pf}	specific heat of air (J/(kg·K))
d_p	diameter of solid particle (m)
e_f	internal energy of air (J/kg)
e_p	internal energy of solid particle (J/kg)
E_{fp}	volumetric energy exchange between air and solid particles (W/m^3)
E_{fp}	volumetric energy exchange between solid particles and air (W/m^3)
E_p	equivalent emission of the particles (W/m^2)
F_{bf}	bulk force on the air (N)
F_{bp}	bulk force on solid particles (N)
F_{fp}	interaction force between air and solid particles (N/m^3)
F_{pf}	interaction force between solid particles and air (N/ m^3)
F_{sf}	surface force on the air (N/m^3)
F_{sp}	surface force on solid particles (N/m^3)
f_{pn}	scattering factor associated with the n^{th} particle.
G	incident radiation (W/m^2)
G_b	turbulence kinetic energy due to buoyancy (W/m^3)
G_k	turbulence kinetic energy due to the mean velocity gradients (W/m^3)
h_{fp}	volumetric heat transfer coefficient between air and solid particles($W/(m^3·K)$)
k_f	thermal conductivity of the air (W/(m·K))
N	the number of solid particles in control volume
n	refractive index of the medium
Nu	Nusselt number
P_f	air pressure (Pa)
Q_{air}	the amount of heat absorbed by air (W)
Q_{cf}	net heat flux into the control plane of the air (W/m^2)
Q_{cp}	net heat flux into the control plane of particles (W/m^2)
Q_{total}	the total energy injected into the receiver (W)
Re	Reynolds number
S_k	source terms (W/m^3)
S_ε	source terms (W/m^3)
T_{pn}	temperature of the n^{th} solid particle (K)
u_f	velocity of the air (m/s)
u_p	velocity of solid particles(m/s)

V	control volume (m^3)
Y_m	contribution of fluctuating dilatation in compressible turbulence to the overall dissipation rate (W/m^3)
z_p	volume fraction of solid particles
Greek	
α	absorption coefficient of solid particle
α_p	equivalent absorption coefficient of solid particle
ε_{pn}	emissivity of the n^{th} solid particle
η	the transient thermal efficiency of receiver
μ_f	dynamic viscosity of the air (Pa·s)
ρ_f	density of the air (kg/m^3)
σ	Stefan-Boltzmann constant ($W/(m^2 \cdot k^4)$)
σ_k	turbulent Prandtl number for k
σ_p	equivalent particle scattering factor
σ_ε	turbulent Prandtl number for ε
τ_{ij}	Reynolds stress tensor (Pa)
φ	average voidage in the fluidized bed

2. Numerical simulation

2.1. The operating principle of the quartz tube solid particle air receiver

The structure of the quartz tube solid particle air receiver that the numerical simulation bases on is shown in Fig.1 [4].

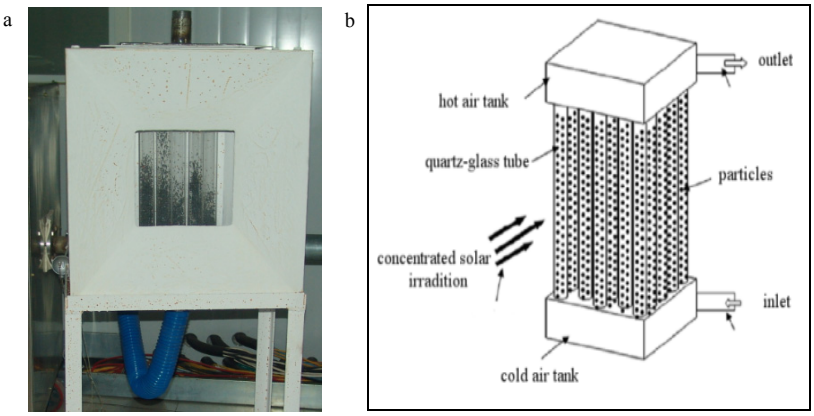

Fig.1. (a) The receiver prototype; (b) The structure of receiver

Before starting up, the solid particles stack at the bottom of the quartz tube. During the operation, the ambient air is blown into tube by the fan or air compressor to make the particles fluidized. The fluidized particles are exposed to the concentrated solar radiation that passes through the quartz wall. The solar energy is absorbed by the dark particles and transferred to the flowing air. Then the hot air comes out from the top of the quartz tube. In this article, the CFD software is utilized to simulate the operation of single quartz tube solid particle air receiver, including the gas-solid flow and heat transfer between them. The single quartz tube used in the numerical simulation is 0.5m in length, 0.04m in outer diameter and 0.003m in wall thickness.

2.2. Governing equations

A three dimensional CFD numerical simulation was performed to simulate the quartz tube solid particle air receiver. According to the volume fraction of solid particles in the receiver, Eulerian Model was selected in the numerical simulation. The equations of continuity, momentum and energy of both air and solid particles are listed as follows [5].

Equations of air:

Continuity equation:

$$\frac{\partial}{\partial t}[(1-z_p)\rho_f]+\frac{\partial}{\partial x^i}[(1-z_p)\rho_f u_f^i]=0 \tag{1}$$

Momentum equation:

$$(1-z_p)\rho_f\frac{\partial u_f^i}{\partial t}+(1-z_p)\rho_f u_f^j\frac{\partial u_f^i}{\partial x^j}=-\frac{\partial p_f}{\partial x^i}+\frac{\partial \tau_f^{ij}}{\partial x^j}+F_{bf}^i+F_{fp}^i \tag{2}$$

Energy equation:

$$\frac{\partial}{\partial t}[(1-z_p)\rho_f(e_f+\frac{1}{2}u_f^iu_f^i)]+\frac{\partial}{\partial x^j}[(1-z_p)\rho_f u_f^j(e_f+\frac{1}{2}u_f^iu_f^i)+F_{sf}^ju_f^j+Q_{cf}^j]=E_{fp}+F_{bf}^ju_f^j \tag{3}$$

Equations of solid particles:

Continuity equation:

$$\frac{\partial}{\partial t}[z_p\rho_p]+\frac{\partial}{\partial x^i}[z_p\rho_p u_p^i]=0 \tag{4}$$

Momentum equation:

$$z_p\rho_p\frac{\partial u_p^i}{\partial t}+z_p\rho_p u_p^j\frac{\partial u_p^i}{\partial x^j}=-\frac{\partial p_p}{\partial x^i}+\frac{\partial \tau_p^{ij}}{\partial x^j}+F_{bp}^i+F_{pf}^i \tag{5}$$

Energy equation:

$$\frac{\partial}{\partial t}[z_p\rho_p(e_p+\frac{1}{2}u_p^iu_p^i)]+\frac{\partial}{\partial x^j}[z_p\rho_p u_p^j(e_p+\frac{1}{2}u_p^iu_p^i)+F_{sp}^ju_p^j+Q_{cp}^j]=E_{pf}+F_{bp}^ju_p^j \tag{6}$$

As for the dense gas-solid turbulent flow in the simulation, standard k-epsilon model was more suitable to conduct the simulation. The equations of standard k-epsilon model are as follows [6].

$$\frac{\partial}{\partial t}(\rho k)+\frac{\partial}{\partial x_i}(\rho k u_i)=\frac{\partial}{\partial x_j}[(\mu+\frac{\mu_t}{\sigma_k})\frac{\partial k}{\partial x_j}]+G_k+G_b-\rho\varepsilon-Y_M+S_k \tag{7}$$

$$\frac{\partial}{\partial t}(\rho\varepsilon)+\frac{\partial}{\partial x_i}(\rho\varepsilon u_i)=\frac{\partial}{\partial x_j}[(\mu+\frac{\mu_t}{\sigma_\varepsilon})\frac{\partial \varepsilon}{\partial x_j}]+C_{1\varepsilon}\frac{\varepsilon}{k}(G_k+C_{3\varepsilon}G_b)-C_{2\varepsilon}\rho\frac{\varepsilon^2}{k}+S_\varepsilon \tag{8}$$

The solid particles played an important role in absorbing and scattering the concentrated solar radiation in the quartz tube solid particle air receiver while the air was considered to be a non-absorbing media. Thus, the P-1 radiation model that ignores the air radiation is presented as the following equations [7-8].

$$\nabla \cdot (\Gamma \nabla G) + 4\pi \left(\alpha n^2 \frac{\sigma T^4}{\pi} + E_p \right) - (\alpha + \alpha_p) G = 0 \tag{9}$$

The definitions of the relative parameters in Eq. 9 are as the following.

$$\Gamma = \frac{1}{3(\alpha + \alpha_p + \sigma_p)} \tag{10}$$

$$E_p = \lim_{V \to 0} \sum_{n=1}^{N} \varepsilon_{pn} A_{pn} \frac{\sigma T_{pn}^4}{\pi V} \tag{11}$$

$$\alpha_p = \lim_{V \to 0} \sum_{n=1}^{N} \varepsilon_{pn} \frac{A_{pn}}{V} \tag{12}$$

$$\sigma_p = \lim_{V \to 0} \sum_{n=1}^{N} (1 - f_{pn})(1 - \varepsilon_{pn}) \frac{A_{pn}}{V} \tag{13}$$

$$A_{pn} = \frac{\pi d_{pn}^2}{4} \tag{14}$$

The hot solid particles transfer heat to the flowing air effectively during the operation of the receiver where the hot air comes out of the outlet. Gunn model is frequently used for Eulerian multiphase simulations, especially for dense gas-solid simulation. In order to simulate the heat transfer between solid particles and the air, Gunn model was utilized in the simulation. The equations of Gunn model are as follows [9].

$$Nu_{fp} = (7 - 10\varphi + 5\varphi^2)(1 + 0.7\,\mathrm{Re}^{0.2}\,\mathrm{Pr}^{1/3}) + (1.33 - 2.4\varphi + 1.2\varphi^2)\,\mathrm{Re}^{0.7}\,\mathrm{Pr}^{1/3} \tag{15}$$

where $Nu_{fp} = h_{fp} d_p / k_f$, $\mathrm{Re} = \left| u_f - u_p \right| d_p \rho_f / \mu_f$, $\mathrm{Pr} = c_{p_f} \mu_f / k_f$, respectively.

2.3. Numerical procedure

The numerical simulation involves complex multiphase flow and convective and radiative heat transfer. Therefore, the main assumptions are given as the following.

(1) The air is incompressible and Newtonian fluid, the air density varies with temperature.
(2) The solid phase consists of spherical particles with uniform diameter and cannot react with oxygen.
(3) The concentrated solar radiation is uniform and the incident direction is normal to the quartz tube wall.
(4) The absorption coefficient of solid particles is independent with the wavelength of incident radiation.
(5) The thermal conductivity in the tube wall is neglected.

The numerical models used in the simulation have been mentioned above and incident radiation is simulated by Solar Ray Tracing model in Ansys Fluent. The quartz tube geometry is meshed by hexahedron with the grid number of 47250. Two cases with different direct solar radiation are simulated. Further, the initial parameters in the numerical simulations are listed in Table 1.

Table1. The initial parameters in the numerical simulations

Parameter	Value
Direct solar radiation-1 (kW/m^2)	600
Direct solar radiation-2(kW/m^2)	1200
Solid particle name	SiC
Diameter of solid particle (mm)	3
Inlet air velocity(m/s)	1.5
Inlet air temperature(K)	293
Packed height of particles (mm)	70
Glass transmissivity of visible	0.9
Glass transmissivity of infrared	0.1
Ambient temperature(K)	293
Convective coefficient on outer wall (W/(m^2·K))	8
External emissivity	0.9
Time step size(s)	0.001
Gravitational Acceleration(m/s^2)	9.81

The size of solid particles in the receiver is much larger and thus the velocity should be higher in order to make the solid particles fluidized. The solid particles may be blown out of the tube, so the initial particles packed height is much lower than the tube length. The fluidized particles concentrate in the lower part of the tube and volume fraction of solid particles in this region is more than 20%. Because of the complexities of dense gas-solid turbulent flow, convective and radiative heat transfer processes in the tube, the time step size is set to 0.001s and the residual of continuity, velocity and energy are 10^{-3}. According to the parameters mentioned in Table.1, the numerical simulation lasted for more than 5 minutes. The temperature of solid and air became steady after being simulated for 5 minutes. Results and discussions are listed as follows.

3. Results and discussions

3.1. Distribution and analysis of temperature

Fig. 2(a) shows that the direct solar radiation injects into the receiver from positive Y-axis. The direct solar radiation distributed on the positive Y-axis tube wall was much higher than that on other walls. The phase distribution of solid particles in the receiver after being simulated for 5 minutes is as shown in Fig. 2(b). Most fluidized particles concentrated in the lower part of the tube. The Z-coordinate of the highest solid phase plane was less than 0.15m. Thus, most of the heat was transferred from solid particles to air in the lower part of the tube.

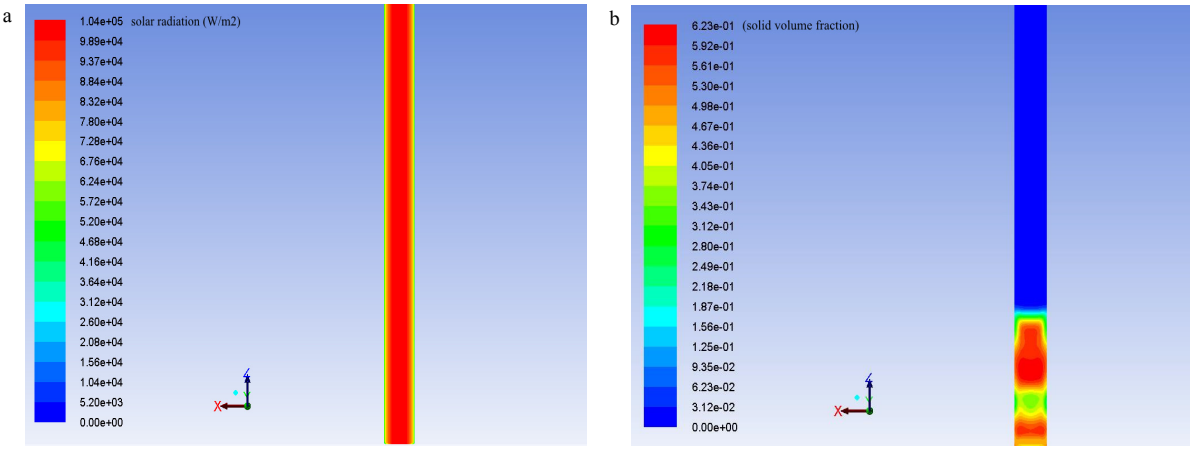

Fig. 2. (a)The distribution of solar radiation on the tube wall (b) The distribution of solid particles in the tube

Fig. 3 and Fig. 4 show distributions of air and solid particles temperature in the tube under different direct solar radiation conditions. The distributions of air and solid particles temperature were uniform in the lower region of the tube. Most fluidized solid particles concentrated in the lower region of the tube and the air and solid exchanged heat effectively in this region. The temperature of air and solid in Fig. 4 were much higher than that shown in Fig. 3, which was due to higher direct solar radiation. In the upper region of the tube, there was almost no solid particle and the temperature of air distributed less uniformly. The air temperature closing to the tube wall was higher than that in the center of receiver because of the higher tube wall temperature partly. As for the rise of the air temperature in the upper region of tube, more research needs to be done in the future. Further, the air temperature distributed comparatively less uniformly along the Y-axis than that distributed along X-axis as the concentrate solar radiation injected into the receiver from positive Y-axis.

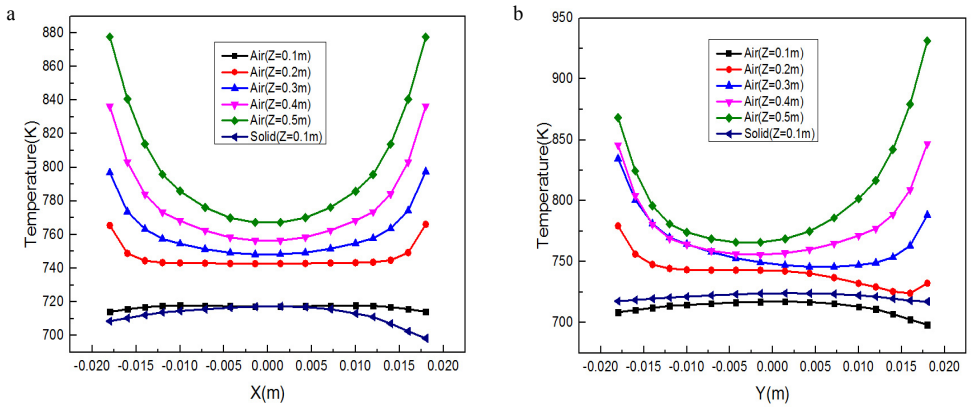

Fig. 3. The distributions of air and solid particles temperature (a) along X-axis and (b) Y-axis at different Z-axis planes (600 kW/m^2)

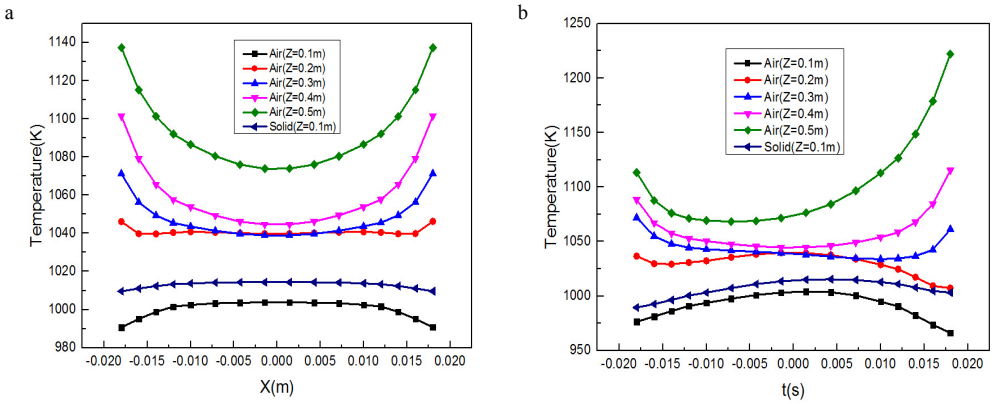

Fig. 4. The distributions of air and solid particles temperature (a) along X-axis and (b) Y-axis at different Z-axis planes (1200 kW/m^2)

3.2. Analysis of thermal performance

In order to get higher outlet air temperature, it is necessary to enhance heat transfer efficiency between solid particles and air. As Fig. 5 showed, the average temperature difference between solid particles and air was less than 25K in both two cases, which indicated that the heat transfer between solid particles and air was very effective. As simulating time went by, the temperature difference between two phases became steady. Compared with direct solar radiation of 1200 kW/m^2, the lower the direct solar radiation resulted in the less temperature difference between two phases.

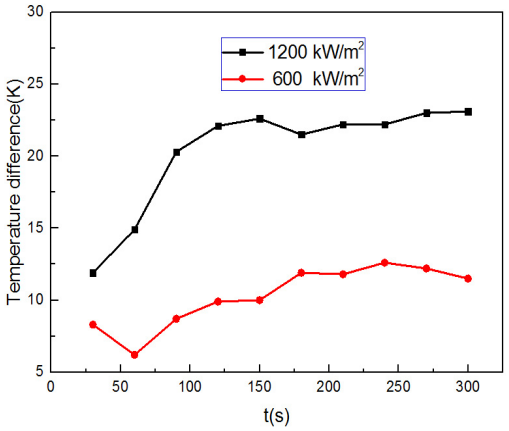

Fig. 5. The volumetric average temperature difference between two phases

The transient thermal efficiency of the quartz tube solid particle air receiver is defined as given.

$$\eta = \frac{Q_{air}}{Q_{total}} \tag{16}$$

Fig. 6 showed the detailed analysis of thermal performance in single tube solid particle air receiver, including average outlet air temperature and transient thermal efficiency of receiver. In the condition of direct solar radiation 600kW/m^2, the average outlet air temperature was more than 800K and the thermal efficiency was about 76.7% after being simulated for 5 minutes. The average outlet air temperature was close to 1100K in the condition of direct solar

radiation 1200kW/m^2 but thermal efficiency decreased to 64.4%. When the direct solar radiation increased, the outlet average air temperature increased while the thermal efficiency decreased. Moreover, the tube wall temperature became higher in the condition of direct solar radiation 1200 kW/m^2, which caused more heat loss to environment through radiative and convective heat transfer. The total proportions of radiative and convective heat losses to the environment were 13.3% in condition of direct solar radiation 600kW/m^2 and 25.6% in the condition of direct solar radiation 1200kW/m^2. About 10% of direct solar radiation was reflected by the tube wall. In order to improve the thermal efficiency of the receiver, it is crucial to reduce the heat loss to the environment. In addition, the maximum tube wall temperature in these cases is 1284.1K, which is lower than temperature limit of quartz glass. The analysis of thermal performance provided important reference for making improvements about the receiver later.

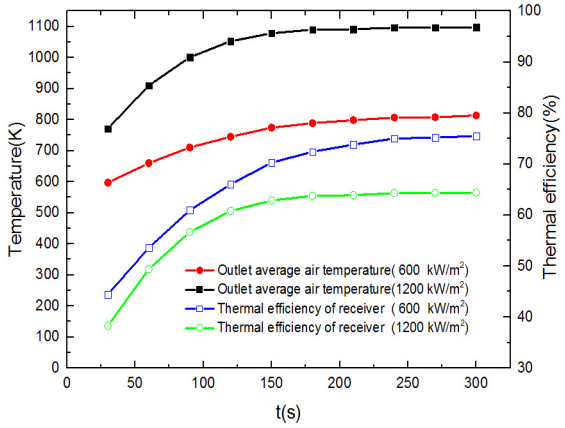

Fig. 6. The detailed analysis of efficiency in the receiver

3.3. Analysis of various velocity conditions

Fig. 7 shows detailed thermal analysis of various inlet air velocity conditions. The direct solar radiation applied in these simulations was 600kW/m^2. As the velocity increased, the average outlet air temperature decreased while the transient thermal efficiency of receiver in the fluidized region increased. The higher velocity contributed to the more effective heat transfer between solid particles and air. Thus, the temperature of solid particles could not rise to a high level, which caused that the average air temperature became lower. However, the air mass flow rate in higher velocity condition became larger and thus the air could transfer more heat with solid particles in the same time period, improving the efficiency of the receiver in the fluidized region. Moreover, it is significant to set up a proper inlet air velocity so that the particles can be fluidized steadily. Thereby, the outlet air temperature and transient-thermal efficiency of the receiver can change smoothly, which is beneficial for the operation of the entire solar power plant.

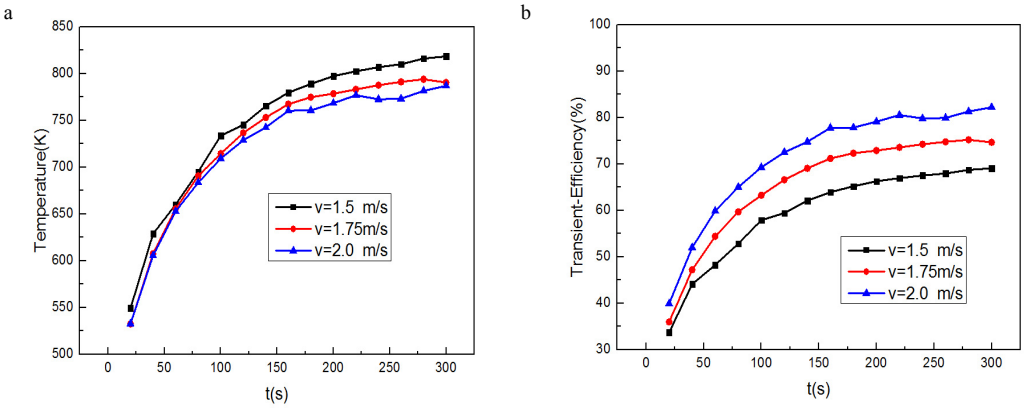

Fig. 7 (a). The average outlet air temperature; (b) Transient-thermal efficiency of the receiver

4. Conclusions

According to the numerical simulation of single quartz tube solid particle air receiver, the following conclusions are obtained.

(1) The temperature of both solid particles and air distribute uniformly in the region where fluidized particles concentrate. For the upper region of tube where fluidized particles become dilute, the air temperature closing to the tube wall is higher than that in the center of receiver.

(2) The temperature difference between air and solid particles is less than 25K, indicating the heat transfer between solid particles and air is very effective.

(3) With the increase of direct solar thermal radiation, the average air temperature in the outlet increases while the transient thermal efficiency decreases. It is important to reduce the radiative and convective heat loss to the environment caused by high tube wall temperature.

(4) With the increasing air inlet velocity, the averaging air temperature in the outlet decreases while the transient thermal efficiency of the receiver in the fluidized region increases. The air inlet velocity is important to ensure that the receiver can be operated in a steady way.

Acknowledgements

This work is financially supported by National Natural Scientific Foundation of China (Gran No. 51376716) and the National High-tech R&D Program (863 Program) of China (No.2012AA050603).

References

[1] Kolb G J, Ho C K, Mancini T R, et al. Power tower technology roadmap and cost reduction plan [J]. SAND2011-2419, Sandia National Laboratories, Albuquerque, NM, 2011.
[2] Hsieh H-T, Siegel N. Computational fluid dynamics modeling of gas-particle flow within a solid-particle solar receiver [J]. Journal of solar energy engineering, 2007, 129(2): 160-170.
[3] Siegel N P, Ho C K, Khalsa S S, et al. Development and evaluation of a prototype solid particle receiver: on-sun testing and model validation. Journal of solar energy engineering, 2010, 132(2).
[4] F. Bai, Y. Zhang, X. Zhang, F. Wang,Y. Wang, Z. Wang. Thermal performance of a quartz tube solid particle air receiver. Proceedings of the 2013 SolarPACES Conference, Las Vegas, NV, Sep 17–20, 2013.
[5] S.I. Pai, Two-Phase Flow, Vieweg-Verlag, Braunschweig, 1977.
[6] B. E. Launder and D. B. Spalding. Lectures in Mathematical Models of Turbulence. Academic Press, London, England. 1972.
[7] P. Cheng. "Two-Dimensional Radiating Gas Flow by a Moment Method". [J]. 2. 1662–1664. 1964.
[8] R. Siegel and J. R. Howell. "Thermal Radiation Heat Transfer. Hemisphere Publishing Corporation, Washington DC. 1992.
[9] D. J. Gunn. "Transfer of Heat or Mass to Particles in Fixed and Fluidized Beds". [J]. Heat Mass Transfer. 21. 467–476. 1978.